Measurement of Bottom Versus Charm as a Function of Transverse Momentum with Electron-Hadron Correlations in $p + p$ Collisions at $\sqrt{s} = 200$ GeV

A. Adare,[11] S. Afanasiev,[25] C. Aidala,[12,36] N. N. Ajitanand,[53] Y. Akiba,[47,48] H. Al-Bataineh,[42] J. Alexander,[53] K. Aoki,[30,47] L. Aphecetche,[55] R. Armendariz,[42] S. H. Aronson,[6] J. Asai,[47,48] E. T. Atomssa,[31] R. Averbeck,[54] T. C. Awes,[43] B. Azmoun,[6] V. Babintsev,[21] M. Bai,[5] G. Baksay,[17] L. Baksay,[17] A. Baldisseri,[14] K. N. Barish,[7] P. D. Barnes,[33] B. Bassalleck,[41] A. T. Basye,[1] S. Bathe,[7] S. Batsouli,[43] V. Baublis,[46] C. Baumann,[37] A. Bazilevsky,[6] S. Belikov,[6,*] R. Bennett,[54] A. Berdnikov,[50] Y. Berdnikov,[50] A. A. Bickley,[11] J. G. Boissevain,[33] H. Borel,[14] K. Boyle,[54] M. L. Brooks,[33] H. Buesching,[6] V. Bumazhnov,[21] G. Bunce,[6,48] S. Butsyk,[33,54] C. M. Camacho,[33] S. Campbell,[54] B. S. Chang,[62] W. C. Chang,[2] J.-L. Charvet,[14] S. Chernichenko,[21] J. Chiba,[26] C. Y. Chi,[12] M. Chiu,[22] I. J. Choi,[62] R. K. Choudhury,[4] T. Chujo,[58,59] P. Chung,[53] A. Churyn,[21] V. Cianciolo,[43] Z. Citron,[54] C. R. Cleven,[19] B. A. Cole,[12] M. P. Comets,[44] P. Constantin,[33] M. Csanád,[16] T. Csörgő,[27] T. Dahms,[54] S. Dairaku,[30,47] K. Das,[18] G. David,[6] M. B. Deaton,[1] K. Dehmelt,[17] H. Delagrange,[55] A. Denisov,[21] D. d'Enterria,[12,31] A. Deshpande,[48,54] E. J. Desmond,[6] O. Dietzsch,[51] A. Dion,[54] M. Donadelli,[51] O. Drapier,[31] A. Drees,[54] K. A. Drees,[5] A. K. Dubey,[61] A. Durum,[21] D. Dutta,[4] V. Dzhordzhadze,[7] Y. V. Efremenko,[43] J. Egdemir,[54] F. Ellinghaus,[11] W. S. Emam,[7] T. Engelmore,[12] A. Enokizono,[32] H. En'yo,[47,48] S. Esumi,[58] K. O. Eyser,[7] B. Fadem,[38] D. E. Fields,[41,48] M. Finger, Jr.,[8,25] M. Finger,[8,25] F. Fleuret,[31] S. L. Fokin,[29] Z. Fraenkel,[61,*] J. E. Frantz,[54] A. Franz,[6] A. D. Frawley,[18] K. Fujiwara,[47] Y. Fukao,[30,47] T. Fusayasu,[40] S. Gadrat,[34] I. Garishvili,[56] A. Glenn,[11] H. Gong,[54] M. Gonin,[31] J. Gosset,[14] Y. Goto,[47,48] R. Granier de Cassagnac,[31] N. Grau,[12,24] S. V. Greene,[59] M. Grosse Perdekamp,[22,48] T. Gunji,[10] H.-Å. Gustafsson,[35] T. Hachiya,[20] A. Hadj Henni,[55] C. Haegemann,[41] J. S. Haggerty,[6] H. Hamagaki,[10] R. Han,[45] H. Harada,[20] E. P. Hartouni,[32] K. Haruna,[20] E. Haslum,[35] R. Hayano,[10] M. Heffner,[32] T. K. Hemmick,[54] T. Hester,[7] X. He,[19] H. Hiejima,[22] J. C. Hill,[24] R. Hobbs,[41] M. Hohlmann,[17] W. Holzmann,[53] K. Homma,[20] B. Hong,[28] T. Horaguchi,[10,47,57] D. Hornback,[56] S. Huang,[59] T. Ichihara,[47,48] R. Ichimiya,[47] Y. Ikeda,[58] K. Imai,[30,47] J. Imrek,[15] M. Inaba,[58] Y. Inoue,[49,47] D. Isenhower,[1] L. Isenhower,[1] M. Ishihara,[47] T. Isobe,[10] M. Issah,[53] A. Isupov,[25] D. Ivanischev,[46] B. V. Jacak,[54,†] J. Jia,[12] J. Jin,[12] O. Jinnouchi,[48] B. M. Johnson,[6] K. S. Joo,[39] D. Jouan,[44] F. Kajihara,[10] S. Kametani,[10,47,60] N. Kamihara,[47,48] J. Kamin,[54] M. Kaneta,[48] J. H. Kang,[62] H. Kanou,[47,57] J. Kapustinsky,[33] D. Kawall,[36,48] A. V. Kazantsev,[29] T. Kempel,[24] A. Khanzadeev,[46] K. M. Kijima,[20] J. Kikuchi,[60] B. I. Kim,[28] D. H. Kim,[39] D. J. Kim,[62] E. Kim,[52] S. H. Kim,[62] E. Kinney,[11] K. Kiriluk,[11] A. Kiss,[16] E. Kistenev,[6] A. Kiyomichi,[47] J. Klay,[32] C. Klein-Boesing,[37] L. Kochenda,[46] V. Kochetkov,[21] B. Komkov,[46] M. Konno,[58] J. Koster,[22] D. Kotchetkov,[7] A. Kozlov,[61] A. Král,[13] A. Kravitz,[12] J. Kubart,[8,23] G. J. Kunde,[33] N. Kurihara,[10] K. Kurita,[49,47] M. Kurosawa,[47] M. J. Kweon,[28] Y. Kwon,[56,62] G. S. Kyle,[42] R. Lacey,[53] Y.-S. Lai,[12] Y. S. Lai,[12] J. G. Lajoie,[24] D. Layton,[22] A. Lebedev,[24] D. M. Lee,[33] K. B. Lee,[28] M. K. Lee,[62] T. Lee,[52] M. J. Leitch,[33] M. A. L. Leite,[51] B. Lenzi,[51] P. Liebing,[48] T. Liška,[13] A. Litvinenko,[25] H. Liu,[42] M. X. Liu,[33] X. Li,[9] B. Love,[59] D. Lynch,[6] C. F. Maguire,[59] Y. I. Makdisi,[5] A. Malakhov,[25] M. D. Malik,[41] V. I. Manko,[29] E. Mannel,[12] Y. Mao,[45,47] L. Mašek,[8,23] H. Masui,[58] F. Matathias,[12] M. McCumber,[54] P. L. McGaughey,[33] N. Means,[54] B. Meredith,[22] Y. Miake,[58] P. Mikeš,[8,23] K. Miki,[58] T. E. Miller,[59] A. Milov,[6,54] S. Mioduszewski,[6] M. Mishra,[3] J. T. Mitchell,[6] M. Mitrovski,[53] A. K. Mohanty,[4] Y. Morino,[10] A. Morreale,[7] D. P. Morrison,[6] T. V. Moukhanova,[29] D. Mukhopadhyay,[59] J. Murata,[49,47] S. Nagamiya,[26] Y. Nagata,[58] J. L. Nagle,[11] M. Naglis,[61] M. I. Nagy,[16] I. Nakagawa,[47,48] Y. Nakamiya,[20] T. Nakamura,[20] K. Nakano,[47,57] J. Newby,[32] M. Nguyen,[54] T. Niita,[58] B. E. Norman,[33] R. Nouicer,[6] A. S. Nyanin,[29] E. O'Brien,[6] S. X. Oda,[10] C. A. Ogilvie,[24] H. Ohnishi,[47] H. Okada,[30,47] K. Okada,[48] M. Oka,[58] O. O. Omiwade,[1] Y. Onuki,[47] A. Oskarsson,[35] M. Ouchida,[20] K. Ozawa,[10] R. Pak,[6] D. Pal,[59] A. P. T. Palounek,[33] V. Pantuev,[54] V. Papavassiliou,[42] J. Park,[52] W. J. Park,[28] S. F. Pate,[42] H. Pei,[24] J.-C. Peng,[22] H. Pereira,[14] V. Peresedov,[25] D. Yu. Peressounko,[29] C. Pinkenburg,[6] M. L. Purschke,[6] A. K. Purwar,[33] H. Qu,[19] J. Rak,[41] A. Rakotozafindrabe,[31] I. Ravinovich,[61] K. F. Read,[43,56] S. Rembeczki,[17] M. Reuter,[54] K. Reygers,[37] V. Riabov,[46] Y. Riabov,[46] D. Roach,[59] G. Roche,[34] S. D. Rolnick,[7] A. Romana,[31,*] M. Rosati,[24] S. S. E. Rosendahl,[35] P. Rosnet,[34] P. Rukoyatkin,[25] P. Ružička,[23] V. L. Rykov,[47] B. Sahlmueller,[37] N. Saito,[30,47,48] T. Sakaguchi,[6] S. Sakai,[58] K. Sakashita,[47,57] H. Sakata,[20] V. Samsonov,[46] S. Sato,[26] T. Sato,[58] S. Sawada,[26] K. Sedgwick,[7] J. Seele,[11] R. Seidl,[22] A. Yu. Semenov,[24] V. Semenov,[21] R. Seto,[7] D. Sharma,[61] I. Shein,[21] A. Shevel,[46,53] T.-A. Shibata,[47,57] K. Shigaki,[20] M. Shimomura,[58] K. Shoji,[30,47] P. Shukla,[4] A. Sickles,[6,54] C. L. Silva,[51] D. Silvermyr,[43] C. Silvestre,[14] K. S. Sim,[28] B. K. Singh,[3] C. P. Singh,[3] V. Singh,[3] S. Skutnik,[24] M. Slunečka,[8,25] A. Soldatov,[21] R. A. Soltz,[32] W. E. Sondheim,[33] S. P. Sorensen,[56] I. V. Sourikova,[6] F. Staley,[14] P. W. Stankus,[43] E. Stenlund,[35] M. Stepanov,[42] A. Ster,[27] S. P. Stoll,[6] T. Sugitate,[20] C. Suire,[44] A. Sukhanov,[6] J. Sziklai,[27] T. Tabaru,[48] S. Takagi,[58] E. M. Takagui,[51] A. Taketani,[47,48]

R. Tanabe,[58] Y. Tanaka,[40] K. Tanida,[47,48] M. J. Tannenbaum,[6] A. Taranenko,[53] P. Tarján,[15] H. Themann,[54] T. L. Thomas,[41] M. Togawa,[30,47] A. Toia,[54] J. Tojo,[47] L. Tomášek,[23] Y. Tomita,[58] H. Torii,[20,47] R. S. Towell,[1] V-N. Tram,[31] I. Tserruya,[61] Y. Tsuchimoto,[20] C. Vale,[24] H. Valle,[59] H. W. van Hecke,[33] A. Veicht,[22] J. Velkovska,[59] R. Vertesi,[15] A. A. Vinogradov,[29] M. Virius,[13] V. Vrba,[23] E. Vznuzdaev,[46] M. Wagner,[30,47] D. Walker,[54] X. R. Wang,[42] Y. Watanabe,[47,48] F. Wei,[24] J. Wessels,[37] S. N. White,[6] D. Winter,[12] C. L. Woody,[6] M. Wysocki,[11] W. Xie,[48] Y. L. Yamaguchi,[60] K. Yamaura,[20] R. Yang,[22] A. Yanovich,[21] Z. Yasin,[7] J. Ying,[19] S. Yokkaichi,[47,48] G. R. Young,[43] I. Younus,[41] I. E. Yushmanov,[29] W. A. Zajc,[12] O. Zaudtke,[37] C. Zhang,[43] S. Zhou,[9] J. Zimányi,[27,*] and L. Zolin[25]

(PHENIX Collaboration)

[1]*Abilene Christian University, Abilene, Texas 79699, USA*
[2]*Institute of Physics, Academia Sinica, Taipei 11529, Taiwan*
[3]*Department of Physics, Banaras Hindu University, Varanasi 221005, India*
[4]*Bhabha Atomic Research Centre, Bombay 400 085, India*
[5]*Collider-Accelerator Department, Brookhaven National Laboratory, Upton, New York 11973-5000, USA*
[6]*Physics Department, Brookhaven National Laboratory, Upton, New York 11973-5000, USA*
[7]*University of California - Riverside, Riverside, California 92521, USA*
[8]*Charles University, Ovocný trh 5, Praha 1, 116 36, Prague, Czech Republic*
[9]*China Institute of Atomic Energy (CIAE), Beijing, People's Republic of China*
[10]*Center for Nuclear Study, Graduate School of Science, University of Tokyo, 7-3-1 Hongo, Bunkyo, Tokyo 113-0033, Japan*
[11]*University of Colorado, Boulder, Colorado 80309, USA*
[12]*Columbia University, New York, New York 10027 and Nevis Laboratories, Irvington, New York 10533, USA*
[13]*Czech Technical University, Zikova 4, 166 36 Prague 6, Czech Republic*
[14]*Dapnia, CEA Saclay, F-91191, Gif-sur-Yvette, France*
[15]*Debrecen University, H-4010 Debrecen, Egyetem tér 1, Hungary*
[16]*ELTE, Eötvös Loránd University, H - 1117 Budapest, Pázmány P. s. 1/A, Hungary*
[17]*Florida Institute of Technology, Melbourne, Florida 32901, USA*
[18]*Florida State University, Tallahassee, Florida 32306, USA*
[19]*Georgia State University, Atlanta, Georgia 30303, USA*
[20]*Hiroshima University, Kagamiyama, Higashi-Hiroshima 739-8526, Japan*
[21]*IHEP Protvino, State Research Center of Russian Federation, Institute for High Energy Physics, Protvino, 142281, Russia*
[22]*University of Illinois at Urbana-Champaign, Urbana, Illinois 61801, USA*
[23]*Institute of Physics, Academy of Sciences of the Czech Republic, Na Slovance 2, 182 21 Prague 8, Czech Republic*
[24]*Iowa State University, Ames, Iowa 50011, USA*
[25]*Joint Institute for Nuclear Research, 141980 Dubna, Moscow Region, Russia*
[26]*KEK, High Energy Accelerator Research Organization, Tsukuba, Ibaraki 305-0801, Japan*
[27]*KFKI Research Institute for Particle and Nuclear Physics of the Hungarian Academy of Sciences (MTA KFKI RMKI), H-1525 Budapest 114, Post Office Box 49, Budapest, Hungary*
[28]*Korea University, Seoul, 136-701, Korea*
[29]*Russian Research Center "Kurchatov Institute", Moscow, Russia*
[30]*Kyoto University, Kyoto 606-8502, Japan*
[31]*Laboratoire Leprince-Ringuet, Ecole Polytechnique, CNRS-IN2P3, Route de Saclay, F-91128, Palaiseau, France*
[32]*Lawrence Livermore National Laboratory, Livermore, California 94550, USA*
[33]*Los Alamos National Laboratory, Los Alamos, New Mexico 87545, USA*
[34]*LPC, Université Blaise Pascal, CNRS-IN2P3, Clermont-Fd, 63177 Aubiere Cedex, France*
[35]*Department of Physics, Lund University, Box 118, SE-221 00 Lund, Sweden*
[36]*Department of Physics, University of Massachusetts, Amherst, Massachusetts 01003-9337, USA*
[37]*Institut für Kernphysik, University of Muenster, D-48149 Muenster, Germany*
[38]*Muhlenberg College, Allentown, Pennsylvania 18104-5586, USA*
[39]*Myongji University, Yongin, Kyonggido 449-728, Korea*
[40]*Nagasaki Institute of Applied Science, Nagasaki-shi, Nagasaki 851-0193, Japan*
[41]*University of New Mexico, Albuquerque, New Mexico 87131, USA*
[42]*New Mexico State University, Las Cruces, New Mexico 88003, USA*
[43]*Oak Ridge National Laboratory, Oak Ridge, Tennessee 37831, USA*
[44]*IPN-Orsay, Universite Paris Sud, CNRS-IN2P3, BP1, F-91406, Orsay, France*
[45]*Peking University, Beijing, People's Republic of China*
[46]*PNPI, Petersburg Nuclear Physics Institute, Gatchina, Leningrad region, 188300, Russia*
[47]*RIKEN Nishina Center for Accelerator-Based Science, Wako, Saitama 351-0198, Japan*
[48]*RIKEN BNL Research Center, Brookhaven National Laboratory, Upton, New York 11973-5000, USA*

[49]Physics Department, Rikkyo University, 3-34-1 Nishi-Ikebukuro, Toshima, Tokyo 171-8501, Japan
[50]Saint Petersburg State Polytechnic University, St. Petersburg, Russia
[51]Universidade de São Paulo, Instituto de Física, Caixa Postal 66318, São Paulo CEP05315-970, Brazil
[52]System Electronics Laboratory, Seoul National University, Seoul, Korea
[53]Chemistry Department, Stony Brook University, Stony Brook, SUNY, New York 11794-3400, USA
[54]Department of Physics and Astronomy, Stony Brook University, SUNY, Stony Brook, New York 11794, USA
[55]SUBATECH (Ecole des Mines de Nantes, CNRS-IN2P3, Université de Nantes) BP 20722 - 44307, Nantes, France
[56]University of Tennessee, Knoxville, Tennessee 37996, USA
[57]Department of Physics, Tokyo Institute of Technology, Oh-okayama, Meguro, Tokyo 152-8551, Japan
[58]Institute of Physics, University of Tsukuba, Tsukuba, Ibaraki 305, Japan
[59]Vanderbilt University, Nashville, Tennessee 37235, USA
[60]Waseda University, Advanced Research Institute for Science and Engineering, 17 Kikui-cho, Shinjuku-ku, Tokyo 162-0044, Japan
[61]Weizmann Institute, Rehovot 76100, Israel
[62]Yonsei University, IPAP, Seoul 120-749, Korea

(Received 29 March 2009; published 18 August 2009)

The momentum distribution of electrons from semileptonic decays of charm and bottom quarks for midrapidity $|y| < 0.35$ in $p + p$ collisions at $\sqrt{s} = 200$ GeV is measured by the PHENIX experiment at the Relativistic Heavy Ion Collider over the transverse momentum range $2 < p_T < 7$ GeV/c. The ratio of the yield of electrons from bottom to that from charm is presented. The ratio is determined using partial $D/\bar{D} \to e^{\pm}K^{\mp}X$ (K unidentified) reconstruction. It is found that the yield of electrons from bottom becomes significant above 4 GeV/c in p_T. A fixed-order-plus-next-to-leading-log perturbative quantum chromodynamics calculation agrees with the data within the theoretical and experimental uncertainties. The extracted total bottom production cross section at this energy is $\sigma_{b\bar{b}} = 3.2^{+1.2}_{-1.1}(\text{stat})^{+1.4}_{-1.3}(\text{syst})\mu b$.

DOI: 10.1103/PhysRevLett.103.082002 PACS numbers: 13.85.Qk, 13.20.Fc, 13.20.He, 25.75.Dw

Measurements of heavy flavor production (charm and bottom) in $p + p$ collisions present stringent tests for perturbative quantum chromodynamics (pQCD) calculations. For instance, while bottom production at the Tevatron is well described by next-to-leading order (NLO) pQCD [1], the cross section for charm production at high p_T, though compatible within the theoretical uncertainties, is higher than the preferred theoretical value by ~50% [2]. Measurement of heavy flavor in $p + p$ collisions also provides an important baseline for study of the medium created in relativistic heavy-ion collisions. The PHENIX experiment at the Relativistic Heavy Ion Collider (RHIC) has measured single electrons from the semileptonic decay of heavy flavor at midrapidity in $p + p$ and Au + Au collisions at $\sqrt{s_{NN}} = 200$ GeV [3,4]. Strong suppression of the single electron yield at high p_T, which includes contributions from both charm and bottom decays, was observed in central Au + Au collisions [4]. This effect is conventionally attributed to energy loss by the parent parton in the medium [5]; one also expects the energy loss suffered by bottom quarks to be significantly less than that suffered by charm quarks due to the difference in their masses [6,7]. Clearly, for both pQCD comparisons and the heavy-ion reference, one wants to disentangle the yields of charm and bottom at RHIC energies.

In this Letter, we present the yield ratio of single electrons from bottom to those from heavy flavor at midrapidity in $p + p$ collisions at $\sqrt{s} = 200$ GeV, using partial $D/\bar{D} \to e^{\pm}K^{\mp}X$ (K unidentified) reconstruction. The data were collected with the PHENIX detector [8] in the 2005 and 2006 RHIC runs using its two central arm spectrometers. Each spectrometer covers $|\eta| < 0.35$ in pseudorapidity and $\Delta\phi = \pi/2$ in azimuth. The arms include drift chambers (DC) and pad chambers (PC1,2,3) for charged particle tracking, a ring imaging Čerenkov detector (RICH) and an electromagnetic calorimeter (EMCal) for electron identification and triggering. Beam-beam counters (BBCs), covering pseudorapidity $3.1 < |\eta| < 3.9$, measure the position of the collision vertex along the beam (z_{vtx}) and provide the interaction trigger. In the 2005 run, helium bags were placed in the space between the beam pipe and DC to reduce photon conversions. The bags were removed in 2006.

Two data sets are used for the analysis: (i) a minimum bias (MB) data set recorded with the BBC trigger, and (ii) an electron enriched sample, recorded with a level-1 "ERT" trigger requiring a combination of EMCal and RICH information in coincidence with the BBC trigger. The BBC trigger cross section is 23.0 ± 2.2 mb [9]. The BBC trigger selects ~53% of inelastic $p + p$ collisions and $(79 \pm 2)\%$ of hard scattering events, such as those with high-p_T particles at midrapidity. The latter efficiency is approximately p_T and particle independent, which was verified by the observed ratio of high-p_T pion and eta yields with and without the BBC trigger, and confirmed with a Monte Carlo simulation [9,10]. After selection of good runs and a vertex cut of $|z_{\text{vtx}}| < 25$ cm, an integrated luminosity ($\int Ldt$) in the ERT data of 1.77 pb^{-1} in the 2005 run and 4.22 pb^{-1} in the 2006 run are used for this analysis.

Charged particle tracks are reconstructed using the DC and PC1. The momentum resolution is ~1% at

$p_T \sim 1$ GeV/c, and the momentum scale is calibrated within 1%. Electron identification (eID) is performed using the RICH and EMCal. The purity of the electron sample is better than 99% for $1 < p_T < 5$ GeV/c [3]. Our previous measurement [3] determined the spectrum of the single electrons from heavy flavor in the 2005 run. Inclusive electron spectra from the 2005 run and the 2006 run are consistent within 5% after taking into account a contribution from the increased photon conversion due to the absence of the helium bags.

The spectrum of the single electrons from heavy flavor is determined using the "cocktail method" [3,4]. The electron spectrum from all known sources except semileptonic decay of heavy flavor is calculated using a Monte Carlo simulation and subtracted from the inclusive spectrum in the cocktail method. The dominant source of background is the π^0 Dalitz decay. The cocktail also includes contributions from quarkonium (J/ψ, Υ) and the Drell-Yan process, which were neglected in our previous measurements [3,4]. These contributions are negligible (smaller than 1% in background) for $p_T < 1$ GeV/c, but become significant at high p_T (above 10% for $p_T > 2.5$ GeV/c) [11]. The signal to background ratio increases with increasing p_T, approaching unity for $p_T \sim 3$ GeV/c [3].

The systematic uncertainties of the inclusive electron spectrum includes the uncertainty in luminosity (9.6%), geometrical acceptance (3%), eID efficiency (2%), and the ERT trigger efficiency (4% at $p_T > 2$ GeV/c). The uncertainty in the cocktail method is p_T dependent (3% at $p_T \sim 2$ GeV/c, increasing to 9% at 9 GeV/c).

The ratio of $(b \to e)$ to $[(c \to e) + (b \to e)]$ is extracted from the correlation between the heavy flavor electrons and associated hadrons [12,13]. The extraction is based on partial reconstruction of the $D/\bar{D} \to e^{\pm}K^{\mp}X$ decay. The invariant mass of unlike charge-sign electron-hadron pairs reveals a correlated signal below the D meson mass of ~ 1.9 GeV/c^2, because of the charge correlation in the D decays. Pairs are formed between a trigger electron ($2.0 < p_T < 7.0$ GeV/c) and an oppositely charged hadron ($0.4 < p_T < 5.0$ GeV/c). The hadron p_T is required to be less than 5 GeV/c, because pions also emit Čerenkov photons in the RICH above 5 GeV/c. The acceptances of positive and negative charged particles are forced to be identical by a geometrical acceptance cut. Since the momentum range of good charged kaon identification is limited, K identification is not performed but the mass of all reconstructed hadrons is set to be that of the K. Most e^+e^- pairs are then removed by an electron veto cut for the hadrons. The reconstructed mass of e^+e^- pairs has a clear peak at low mass. The remaining background e^+e^- pairs are removed by requiring $M_{ee} > 80$ MeV/c^2, where the pair mass is calculated assuming both particles in the pair are electrons.

Depending on the origin of the trigger electrons, the inclusive reconstructed electron-hadron pairs are (i) unlike-sign pairs from charm, (ii) unlike-sign pairs from bottom, (iii) combinatorial background where the electron is a background electron and (iv) background from unlike-sign hadron-hadron pairs due to hadron contamination in the electrons. The main background source is the combinatorial background (iii) and almost all background electrons are from e^+e^- pair creation. Like-sign electron-hadron pairs are used to subtract this background. Since electrons from e^+e^- pair creation and hadrons do not contribute to charge correlated signals, subtraction using like-sign pairs cancels out completely the combinatorial background where the trigger electron is from e^+e^- pair creation (iii). Only the negligibly small (<1%) contribution from K^0_{e3} decay is not canceled out by the subtraction in the background (iii). The contribution from

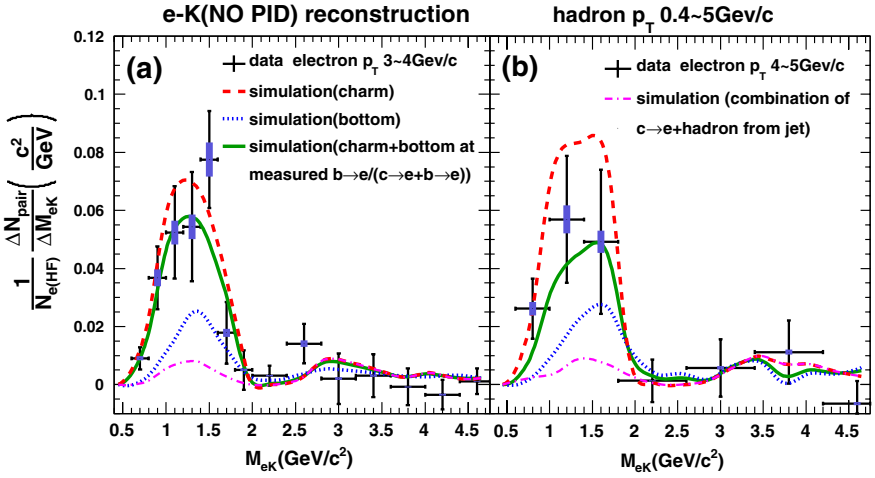

FIG. 1 (color online). Comparison of data to a PYTHIA and EVTGEN [14,15] simulation of the invariant mass distributions in PHENIX acceptance for the reconstructed signal in the 2006 run. The electron p_T range is 3.0–4.0 GeV/c (a) and 4.0–5.0 GeV/c (b). The ratios, $(b \to e)/[(c \to e) + (b \to e)]$, in solid lines are 0.26 (a) and 0.63 (b). Error bars (boxes) indicate statistical (systematic) uncertainties.

hadron contamination (iv) is also less than a 1% effect due to the excellent electron identification. After the subtraction, the reconstructed pairs include a contribution from bottom (ii) due to not identifying K. The contribution from bottom (ii) is much smaller than that from charm (i) due to the bottom decay modes and kinematics. The reconstructed pairs also contain a signal from partial reconstruction of heavy flavor hadrons and a contribution from a combination of heavy flavor electrons and hadrons from jet fragmentation. The ratio of the yield of unlike-sign pairs to that of like-sign pairs is about 1.1 for invariant masses (M_{eK}) below 1.9 GeV/c^2.

The fraction of bottom contribution to the electrons from heavy flavor is obtained as follows:

$$\frac{b \to e}{(c \to e) + (b \to e)} = \frac{\epsilon_c - \epsilon_{\rm data}}{\epsilon_c - \epsilon_b}, \quad (1)$$

where $\epsilon_{\rm data}$ is the tagging efficiency in real data and $\epsilon_{c(b)}$ is the tagging efficiency for charm (bottom) production. These are defined as

$$\epsilon_{\rm data} \equiv \frac{N_{\rm pair}}{N_{e({\rm HF})}} = \frac{N_{c\to{\rm tag}} + N_{b\to{\rm tag}}}{(c \to e) + (b \to e)}, \quad (2)$$

$$\epsilon_c \equiv \frac{N_{c\to{\rm tag}}}{c \to e}, \qquad \epsilon_b \equiv \frac{N_{b\to{\rm tag}}}{b \to e}, \quad (3)$$

where $N_{e({\rm HF})}$ is the number of measured heavy flavor electrons. $N_{\rm pair}$ is the number of background subtracted unlike-sign electron-hadron pairs for invariant mass within $0.4 < M_{eK} < 1.9$ GeV/c^2, which corresponds to the mass range of charmed hadrons. Here, $N_{c(b)\to{\rm tag}}$ is the number of reconstructed signals within $0.4 < M_{eK} < 1.9$ GeV/c^2 for charm (bottom) production.

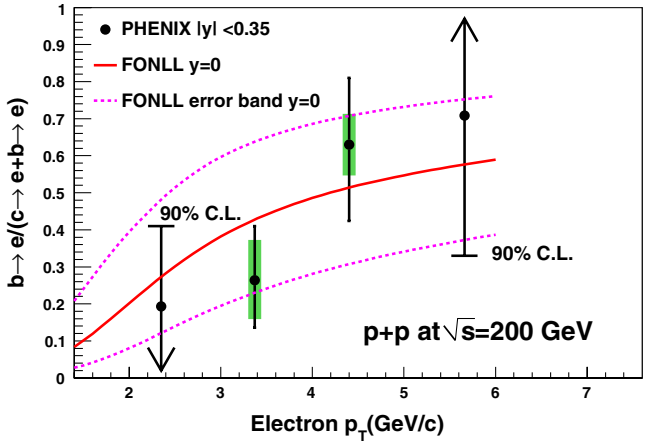

FIG. 2 (color online). $(b \to e)/[(c \to e) + (b \to e)]$ as a function of electron p_T compared to a FONLL calculation [20]. The points show the experimental result. Vertical arrows are used to indicate upper and lower limits. The solid line is a FONLL prediction and the dotted lines represent the uncertainty of this FONLL prediction.

Figure 1 shows the M_{eK} distribution of the reconstructed signals, which is normalized by the yield of heavy flavor electrons ($N_{e({\rm HF})}$) in the range $3 < p_T < 4$ GeV/c [panel (a)] and $4 < p_T < 5$ GeV/c [panel (b)]. The tagging efficiency in real data, $\epsilon_{\rm data}$, is determined by the integration of the M_{eK} distribution in Fig. 1 from $M_{eK} = 0.4$ to 1.9 GeV/c^2 as a function of electron p_T.

The tagging efficiencies for charm and bottom production, ϵ_c and ϵ_b, are calculated with the combination of PYTHIA and EVTGEN [14,15]. PYTHIA is used to simulate charm and bottom production in $p + p$ collisions at $\sqrt{s} =$ 200 GeV and is tuned to reproduce heavy flavor hadron ratios: $D^+/D^0 = 0.45 \pm 0.10$, $D_s/D_0 = 0.25 \pm 0.10$, $\Lambda_c/D^0 = 0.10 \pm 0.05$, $B^+/B^0 = 0.50$, $B_s/B_0 = 0.40 \pm 0.20$, and $B_{\rm baryon}/B^0 = 0.20 \pm 0.15$ [11,16–19]. The Monte Carlo simulation EVTGEN, which is suited for decays of D and B hadrons, is used to simulate the semileptonic decays. The dashed (dotted) lines in Fig. 1 show the M_{eK} distributions of the reconstructed signal for the simulated charm (bottom) production for an electron $3 < p_T < 4$ GeV/c (panel a) and $4 < p_T < 5$ GeV/c [panel (b)]. Some fluctuations in the simulated curves in Fig. 1 come from the limited statistics in the simulation, but the statistical uncertainties in the simulation are negligible compared to that of the data. $\epsilon_{c(b)}$ is determined in the same way as $\epsilon_{\rm data}$ from the M_{eK} distribution for charm (bottom) production. Since about 85% of the extracted

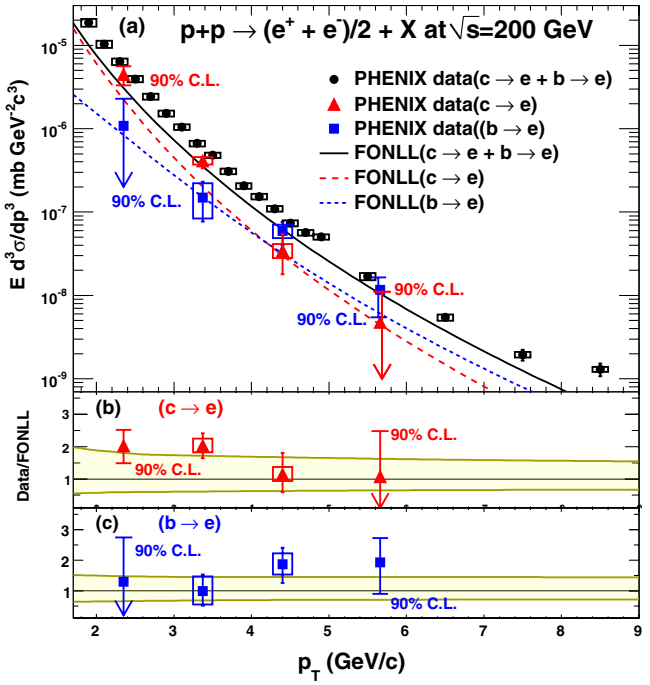

FIG. 3 (color online). (a) Invariant cross sections of electrons from charm and bottom with the FONLL calculation [20]. (b) and (c) The ratios of data points over the FONLL prediction as a function of electron p_T for charm and bottom. The shaded area shows the uncertainty in the FONLL prediction.

signal comes from partial reconstruction of heavy flavor hadrons, the tagging efficiency is determined largely by decay kinematics and $\epsilon_{c(b)}$ can be determined with good precision. The dot-dash lines in Fig. 1 show the contribution from the combination of an electron from charm and hadrons from jet fragmentation for charm production. The solid line in Fig. 1 shows the sum of the M_{eK} distributions for charm and bottom in the simulation with the ratio, $(b \to e)/[(c \to e) + (b \to e)]$, obtained with Eq. (1).

Systematic uncertainties are categorized into two parts related to (i) ϵ_{data} in the real data analysis and (ii) ϵ_c and ϵ_b in the simulation study. The dominant uncertainty in $\epsilon_{\rm data}$ is the uncertainty in the number of heavy flavor electrons (~10%). Uncertainty in $\epsilon_{\rm data}$ also includes a background subtraction uncertainty (1%–10%, p_T dependent). Category (2) includes the uncertainties in geometrical acceptance (3%) and the event generator (~8% for charm and ~9% for bottom). The event generator uncertainty is based on uncertainties, which are known in the production ratios of heavy flavor hadrons (D^+/D^0, D_s/D^0, etc.), known in the branching ratios [16–19], estimated in the momentum distribution of heavy flavor hadrons and estimated in the PYTHIA parameters.

Figure 2 shows the resulting bottom fraction, $(b \to e)/[(c \to e) + (b \to e)]$ as a function of electron p_T compared to a fixed-order-plus-next-to-leading-log perturbative QCD calculation (FONLL) [20]. In this figure, the points show the measured $(b \to e)/[(c \to e) + (b \to e)]$. For the bins with electron p_T ranges $2 < p_T < 3$ and $5 < p_T < 7$ GeV/c, 90% C.L. and mean values are shown. The solid line shows the central value of the FONLL prediction and the dotted lines show its uncertainty.

In Fig. 3, the single electron spectra for charm and bottom are measured from the ratio, $(b \to e)/[(c \to e) + (b \to e)]$, and the spectrum of the electrons from heavy flavor decays. The top panel shows the resulting single electron spectra from charm (triangles) and bottom (squares) compared to the FONLL predictions [20]. The measured spectrum of single electrons (circles) is also shown for reference. The middle (bottom) panel shows the ratio of the measured cross sections to the FONLL calculation for charm (bottom) production. The shaded area shows the uncertainty in the FONLL prediction. The larger mass makes this uncertainty smaller in the case of bottom quarks. These calculations agree with the data for bottom production within the large theoretical and experimental uncertainty. The same is true for charm within the theoretical uncertainty with a ratio of data/FONLL of ~2. A similar tendency was obtained at the Tevatron [1,2].

The electron spectrum from bottom shown in Fig. 3 is integrated from $p_T = 3$ to 5 GeV/c and gives $4.8^{+1.8}_{-1.6}(\text{stat})^{+1.9}_{-1.8}(\text{syst})$ nb. This spectrum is then extrapolated to $p_T = 0$ using the shape predicted by pQCD. PYTHIA with varying intrinsic k_T ($1.5 < k_T < 10$ GeV/c) and FONLL with varying factorization (μ_F) and renormalization (μ_R) scales ($0.5 < \mu_{F,R}/\sqrt{m^2 + p_T^2} < 2$) are used to evaluate the systematic uncertainty (12%) to this extrapolation. The extrapolation results in a bottom cross section at midrapidity of $d\sigma_{b\bar{b}}/dy\,|_{y=0} = 0.92^{+0.34}_{-0.31}(\text{stat})^{+0.39}_{-0.36}(\text{syst})\mu b$, using a $b \to e$ total branching ratio of 10 ± 1%, calculated using the heavy flavor hadron ratios described above. Using HVQMNR [21] with CTEQ5M [22] parton distribution functions (PDF's) to integrate over rapidity, the total bottom cross section is determined to be $\sigma_{b\bar{b}} = 3.2^{+1.2}_{-1.1}(\text{stat})^{+1.4}_{-1.3}(\text{syst})\mu b$. Various PDF's and bottom mass values are used to evaluate the systematic uncertainty (8%) of the rapidity extrapolation. This result is consistent with our result from the dielectron spectrum, which gave $\sigma_{b\bar{b}} = 3.9 \pm 2.5(\text{stat})^{+3}_{-2}(\text{syst})\mu b$ [23]. FONLL predicts $\sigma_{b\bar{b}} = 1.87^{+0.99}_{-0.67}\mu b$, in agreement with both these experimental results.

The fraction of bottom in heavy flavor electrons is found to be larger than 0.33 with 90% confidence level at $p_T > 5$ GeV/c. Furthermore, the assumption of no bottom suppression directly leads to a lower limit on the nuclear modification factor of single electrons, R_{AA}, of greater than 0.33 with the same confidence level. However, according to our measurements, R_{AA} is $\sim 0.25 \pm 0.05(\text{stat}) \pm 0.05(\text{syst})$ at $5 < p_T < 6$ GeV/c [4] in the 0–10% central Au + Au collisions. At the same time the current level of uncertainty in the measurement precludes us from placing significant limits on the possible energy loss of bottom quarks.

In conclusion, the ratio of the yield of electrons from bottom to that from charm has been measured in $p + p$ collisions at $\sqrt{s} = 200$ GeV. The ratio provides the first measurement of the spectrum of electrons from bottom at RHIC. FONLL calculations [20] agree with this result, which provides an important baseline for the study of heavy quark production in the hot and dense matter created in Au + Au collisions.

We thank the staff of the Collider-Accelerator and Physics Departments at BNL for their vital contributions. We acknowledge support from the Office of Nuclear Physics in DOE Office of Science, NSF and a sponsored research grant from Renaissance Technologies (USA), MEXT and JSPS (Japan), CNPq and FAPESP (Brazil), NSFC (China), MSMT (Czech Republic), IN2P3/CNRS, and CEA (France), BMBF, DAAD, and AvH (Germany), OTKA (Hungary), DAE (India), ISF (Israel), KRF and KOSEF (Korea), MES, RAS, and FAAE (Russia), VR and KAW (Sweden), U.S. CRDF for the FSU, US-Hungary Fulbright, and US-Israel BSF.

*Deceased.
†PHENIX spokesperson.
jacak@skipper.physics.sunysb.edu

[1] D. Acosta *et al.*, Phys. Rev. D **71**, 032001 (2005).

[2] D. Acosta *et al.*, Phys. Rev. Lett. **91**, 241804 (2003).
[3] A. Adare *et al.*, Phys. Rev. Lett. **97**, 252002 (2006).
[4] S. S. Adler *et al.*, Phys. Rev. Lett. **98**, 172301 (2007).
[5] M. Gyulassy and M. Plumer, Phys. Lett. B **243**, 432 (1990).
[6] Y. L. Dokshitzer and D. E. Kharzeev, Phys. Lett. B **519**, 199 (2001).
[7] H. van Hees, M. Mannarelli, V. Greco, and R. Rapp, Phys. Rev. Lett. **100**, 192301 (2008).
[8] K. Adcox *et al.*, Nucl. Instrum. Methods Phys. Res., Sect. A **499**, 469 (2003).
[9] S. S. Adler *et al.*, Phys. Rev. C **75**, 024909 (2007).
[10] S. S. Adler *et al.*, Phys. Rev. Lett. **95**, 202001 (2005).
[11] Y. Morino, arXiv:0903.3504.
[12] C. Albajar *et al.*, Phys. Lett. B **186**, 237 (1987).
[13] A. Mischke *et al.*, J. Phys. G **35**, 104117 (2008).
[14] T. Sjostrand, Comput. Phys. Commun. **82**, 74 (1994).
[15] D. Lange, Nucl. Instrum. Methods Phys. Res., Sect. A **462**, 152 (2001).
[16] D. Acosta *et al.*, Phys. Rev. Lett. **91**, 241804 (2003).
[17] L. Gladilin, arXiv:hep-ex/9912064.
[18] G. Alves *et al.*, Phys. Rev. Lett. **77**, 2388 (1996).
[19] W. M. Yao *et al.*, J. Phys. G **33**, 1 (2006).
[20] M. Cacciari, P. Nason, and R. Vogt, Phys. Rev. Lett. **95**, 122001 (2005); (private communication).
[21] M. L. Mangano *et al.*, Nucl. Phys. B **405**, 507 (1993).
[22] H. L. Lai *et al.*, Eur. Phys. J. C **12**, 375 (2000).
[23] A. Adare *et al.*, Phys. Lett. B **670**, 313 (2009).